Available online at www.sciencedirect.com
SCIENCE DIRECT®
International Journal of Heat and Fluid Flow 24 (2003) 267–277
International Journal of HEAT AND FLUID FLOW
www.elsevier.com/locate/ijhff

Optimization of heat transfer utilizing graph based evolutionary algorithms

Kenneth M. Bryden [a,*], Daniel A. Ashlock [b], Douglas S. McCorkle [a], Gregory L. Urban [a]

[a] Department of Mechanical Engineering, Iowa State University, 3030 H.M. Black Engineering Bldg, Ames, IA 50011-2161, USA
[b] Department of Mathematics, Iowa State University, Ames, IA 50011-2161, USA

Received 7 August 2002; accepted 6 December 2002

Abstract

This paper examines the use of graph based evolutionary algorithms (GBEAs) for optimization of heat transfer in a complex system. The specific case examined in this paper is the optimization of heat transfer in a biomass cookstove utilizing three-dimensional computational fluid dynamics to generate the fitness function. In this stove hot combustion gases are used to heat a cooking surface. The goal is to provide an even spatial temperature distribution on the cooking surface by redirecting the flow of combustion gases with baffles. The variables in the optimization are the position and size of the baffles, which are described by integer values. GBEAs are a novel type of EA in which a topology or geography is imposed on an evolving population of solutions. The choice of graph controls the rate at which solutions can spread within the population, impacting the diversity of solutions and convergence rate of the EAs. In this study, the choice of graph in the GBEAs changes the number of mating events required for convergence by a factor of approximately 2.25 and the diversity of the population by a factor of 2. These results confirm that by tuning the graph and parameters in GBEAs, computational time can be significantly reduced.

Keywords: Optimization; Graph based evolutionary algorithm; Computational fluid dynamics; Cookstove; Effectiveness

1. Introduction

Optimization techniques that search a solution space without designer intervention have become important tools in the engineering of many thermal fluid systems. Evolutionary algorithms (EAs) are among the most robust of these optimization methods because the ability to optimize many designs simultaneously makes EAs less susceptible to premature convergence than comparable gradient search methods (Goldberg, 1989). Inspired by biology, EAs evolve populations of designs to explore the solution space. When implemented correctly, EAs are effective at finding good solutions to complex problems and require less knowledge of the solution a priori than other search algorithms. However, a large initial population of random designs and many evolutionary steps are required by EAs to find an acceptable solution. Because of this, EAs tend to be slow and computationally expensive. Application of EAs to thermal systems has been successful in applications where the system or system components can be modeled simplistically through basic thermodynamic equations, curve fits, or other simplified modeling techniques. However, because of the time needed for each fitness call to a computational fluid dynamics (CFD) solver, application of EAs to more complex fluids and heat transfer problems has been limited.

The use of CFD in EAs has been successful in the optimization of some systems with flow pattern based performance. Much of this work has been done in the aircraft industry. Various techniques have been used to reduce the expense, thereby enabling the use of EAs. Typically, reduced versions of the Navier–Stokes equations that can be solved implicitly or by marching are used to reduce the computational expense. The Euler equations or the viscous shock-layer equations (Tannehill et al., 1997) are examples of these equation sets. In other cases, a low detail representation of the actual geometry is used to evolve designs, and a high detail model is used to validate and refine the solution

* Corresponding author. Tel.: +1-515-294-3891; fax: +1-515-294-5530/3261.
E-mail address: kmbryden@iastate.edu (K.M. Bryden).

0142-727X/03/$ - see front matter © 2003 Elsevier Science Inc. All rights reserved.
doi:10.1016/S0142-727X(02)00243-6

Nomenclature

C	normalized encoded description of baffle design	i	cell index
D	diversity (Eq. (2))	q	baffle design component index
F	fitness (Eq. (1))	r	baffle design component index
T	temperature	s	population member index

Subscripts

avg average

(Foster and Dulikravich, 1997; Zha et al., 1997). Using these techniques, researchers have solved several types of problems. These include optimizing airfoils (Mäkinen et al., 1999; Jang and Lee, 2000; Quagliarella and Vicini, 2001), heat exchangers (Fabbri, 1998; Schmit et al., 1996), two-dimensional blade profiles (Trigg et al., 1999), and missile nozzle inlets for high-speed flow (Blaize et al., 1998; Zha et al., 1997). Neural networks have been used to manipulate design structures during evolution by fixing the velocity distribution on the surface of a turbine blade so that only blades meeting the design criteria are considered (Fan, 1998), and used for sensitivity calculations in the evolutionary process (Poloni et al., 2000).

A recently developed evolutionary optimization technique, graph based evolutionary algorithms (GBEA) (Bryden et al., submitted for publication), utilizes population graphing to impose a topology or geography on the evolving solution set. In many cases in nature, the ability of a particular member of a population to mate and reproduce with another is limited. The factors creating these limits vary widely and include geographical distance, mating rituals, and others. The effect of limiting the potential mating pool is a reduced rate of transmission of genetic characteristics and an increased diversity within the populations. A combinatorial graph (or graph) G is a collection $V(G)$ of vertices and $E(G)$ of edges where $E(G)$ is a set of unordered pairs from $V(G)$. The vertices will contain configurations from the evolving population and the edges will designate pairs of vertices that are adjacent, so that reproduction and crossover may take place between them. For additional information on graph theory, the reader is referred to West (1996). By utilizing a graph to impose a geography on the mating population, limits to mating analogous to those observed in nature are created.

In previous studies (Ashlock et al., 1999; Bryden et al., submitted for publication) it was found using simple test problems that the choice of graph in a GBEA can affect the number of mating events required to solve a problem by as much as 12-fold. Also, problems with simpler fitness landscapes performed best with highly connected graphs (10 times faster), while problems with difficult fitness landscapes performed better (12 times faster) with less connected graphs. This occurs because in problems with simple fitness landscapes (e.g., a single hill), the faster the rate of information exchange, the quicker the optimum solution can be identified. In contrast, in complex fitness landscapes a slower rate of information transmittal allows good solutions more time to mature before being challenged by competing good designs. This allows for a more complete exploration of the fitness landscape. A third group of problems that was identified were problems in which the global optimum was composed of the same building blocks as widely scattered and available local optima. The GBEA needs to find a local optima to identify the various building blocks in the solution and then assemble them to create the global optima. In these cases the impact of a graph on the speed of convergence was significantly less, only a 15–20% improvement.

In this study the impact of using GBEAs on a real engineering problem, optimization of a biomass stove, is tested. Specifically, the time to solution and the diversity of the population were examined. Real fluids and heat transfer engineering problems differ from the test problems examined in several ways. These include the time for each system call is minutes or more rather than 1/100 s of a second, the fitness landscape is unknown, the future work may include similar although not identical problems, and the same problem may be revisited with new constraints. Because of this, GBEAs provide a practical means to reduce convergence time.

The engineering problem examined in this paper is the optimization of an improved EcoStove. The EcoStove is a biomass cookstove used in lower income Central American households. It is designed for enhanced efficiency, lower risk of injury, and reduced exposure to harmful emissions. The current stove design needs to be improved because a large temperature variation on the cooking surface limits the effectiveness of the stove for cooking. Field tests have determined that adding baffles to the flow of flue gas from the fire can enhance stove performance; however, the location and size of the baffles for an effective design are unknown.

In this paper, an EAs calling a three-dimensional CFD model of the EcoStove for design assessment is

used to find an optimal flow baffle design. This level of detail is required because there is no simpler, lower cost solver that can predict the surface temperature profile of the stove. The optimization routine consists of the CFD model of the stove and the routines for the GBEA. Star-CD™, a commercial CFD software package, is used to model the stove. Baffle designs are encoded into a simple set of integers that can be manipulated by the GBEA. Because the optimization parameters are integer-valued, gradient based methods are difficult to use. In contrast, EAs can handle integer-valued parameters easily.

2. Background

Nicaragua, like many other developing countries, relies primarily on wood or other biomass fuels for household cooking and heating needs. In 1997 fuelwood represented about 47% of the internal gross primary supply of energy with nearly 90% being consumed for cooking and heating (INE, 1997). Open flame unimproved stoves with low efficiencies were used in more than 95% of homes, resulting in excessive deforestation and high fuel costs (Proleña-Nicaragua, 2000). Additionally, direct exposure to flue gas and biomass residue from inefficient, unventilated stoves has been reported as a significant cause of blindness, cancer, still births, and birth defects (Malhotra, 1999; Barnes et al., 1994; Pandey, 1998; Hong, 1994). Proleña-Nicaragua in conjunction with Aprovecho Research Center, has developed and is distributing in Central America an improved plancha stove, the EcoStove (Fig. 1). The goal of this stove is to provide a single hot spot for quickly boiling water, while maintaining the rest of the stove surface at an even temperature for cooking tortillas or simmering foods. This stove reduces the risk of disease by channeling the flue gas to the outdoors via a duct after heating a cooking surface in an enclosed chamber while maintaining relatively high efficiency. However, the design needs to be improved because the cooking surface has a large temperature variation, with temperatures as cool as 150 °C in some regions and as hot as 600 °C in others. The overall surface temperature is set by the users by varying the fuel feed rate, but the relative spatial temperature variation is unaffected by the fuel rate.

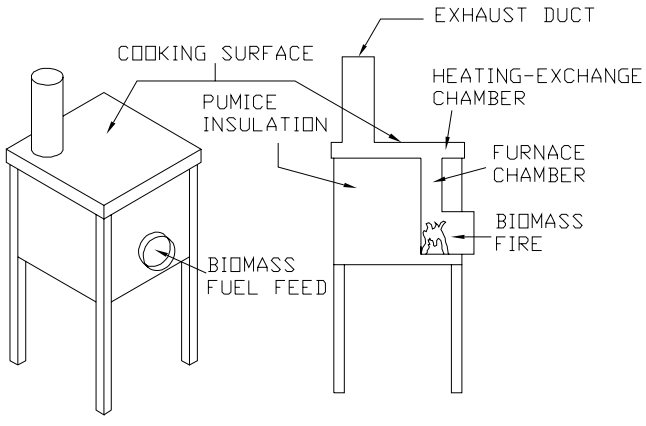

Fig. 1. Schematic of plancha EcoStove.

Attempts to improve the effectiveness of the EcoStove in the field found that extending baffles from the cooking surface into the heating chamber alters the flow in the chamber and the temperature profile of the surface. However, the sophisticated nature of the fluid flow within the heat exchange chamber makes determination of the most effective number of baffles with the correct size, location, and orientation difficult to attain through a ''cut-and-try'' process. Additionally, the baffle stoves must remain easy and inexpensive to manufacture because the tooling and energy resources needed for construction of the handmade stoves are limited. This need is in conflict with the tendency of people to increase the complexity of a design to solve problems encountered during experimental design iteration.

3. The computational model

The geometry of the flow area within the plancha stove is a simple rectangular prism representing the 54 cm × 54 cm × 2.5 cm heat exchange chamber coupled to the furnace chamber and exhaust duct. Combustion within the combustion chamber was not modeled. Instead, the inlet air velocity and temperature conditions were determined from in-field measurements, and the resulting CFD solutions were compared with experimental results. Inlet air with a velocity of 3.88 m/s, a temperature of 977 K, and a density of 0.357 kg/m^3 was found to effectively simulate flue gas leaving the biomass fire chamber. Turbulence was modeled using the K–ϵ model with an intensity of 0.1 and an entrance length of 0.0476 m. Resistance to heat transfer from the cooking surface was modeled using a heat transfer coefficient of 20 W/m^2 K, a thermal conductivity of 30 W/m K, and a surface thickness of 1.6 cm. The remaining surfaces of the model were assumed to be adiabatic to simulate the pumice insulation used in the stove construction. In order to capture two-dimensional heat transfer effects within the plate, use of a model that included three-dimensional heat transfer through the metal plate for a cooking surface was considered. However, including three-dimensional heat transfer in the model significantly increased the convergence time; and the temperature values differed by only a few degrees everywhere on the cooking surface. Full details of the computational model are available in Urban (2001).

Fig. 2 shows the resulting geometry and Fig. 3a shows the CFD solution for the current EcoStove surface profile without baffles. Fig. 3b shows the surface

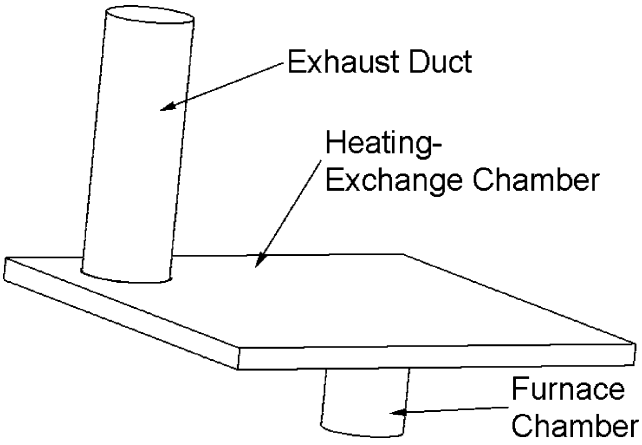

Fig. 2. Geometry used in CFD model.

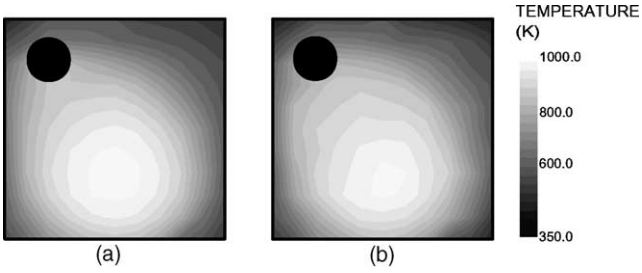

Fig. 3. Predicted (a) and measured (b) temperature distribution for an unbaffled stove.

temperature profile for the unbaffled stove from the experimental data collected in Nicaragua. For each configuration examined, the experimental data was gathered from a locally manufactured stove operated by a Nicaraguan woman for cooking. The fuel feed rate was held constant and the stove was allowed to heat for one and half hours. Following the heatup three sets of data were taken. Each data set required approximately 10 min to collect, and there was a 5 min break between the data sets. Temperatures were taken on a centered 11×11 grid with grid points 5 cm apart. This provides 120 grid points because one point falls in the exhaust chimney. In general the repeatability of the experimental values was good with less than 25 °C difference between repeated measurements. As shown, the agreement between the measured values and the calculated values is excellent. The average temperature difference between the two sets of data is 10 °C. The largest differences between the computational data and the measured data occur in the corners where the computational data predicts a higher temperature than is measured by 20–35 °C. This occurs because three-dimensional conduction to the structural supports is not included in the model. This is acceptable because the cooler corner temperatures do not impact the area available for cooking tortillas or the overall temperature profile of the stove. To ensure that the model was able to accurately predict the temperature profiles of the final designs, following the computational modeling the recommended designs were tested in Nicaragua under the same conditions as the unbaffled stove. Fig. 4a and b show the results of this testing for one of the designs for the calculated and measured data respectively. The average temperature difference between the two sets of data is 13 °C. As with the unbaffled stove the largest temperature differences occur in the corners of the stove. The model accurately predicted both the temperature pattern and the rise in average temperature from the unbaffled stove to the baffled stove (75 °C predicted and 71 °C measured) due to exposing more of the stove surface to the hot combustion gases. The fuel feed rate sets the overall temperature of the stove. The baffled stove reduces fuel consumption in two ways; (1) more of the stove surface is available for cooking, reducing the cooking time, and (2) same average temperature can be achieved with a lower wood feed rate.

The CFD calculations for design evaluations of the EcoStove designs are the most computationally expensive portion of the EA. More than 95% of the computation time is spent running CFD calculations. In general, faster computers have not reduced computation time for CFD solutions because engineers typically exchange the possible time saving for more detailed equation sets or higher resolution grids. More refined solutions are desired because they offer engineers a better understanding of the flow behavior and a better feel for how to improve a system. EAs, however, do not need to gain an understanding of the physics of the problem to find a good solution. Rather, the algorithm only aims to "learn" which pieces of the structure result in designs that better satisfy the fitness criteria. Therefore, the algorithm only requires enough detail in the model to reliably determine which structures are better than others. Because a high resolution CFD model has been verified experimentally, the lowest resolution grid with a solution that reasonably matches the high resolution solution and the field results is the best model for coupling to the EA.

Nine models with different grid resolutions for the EcoStove geometry were created to test for matching

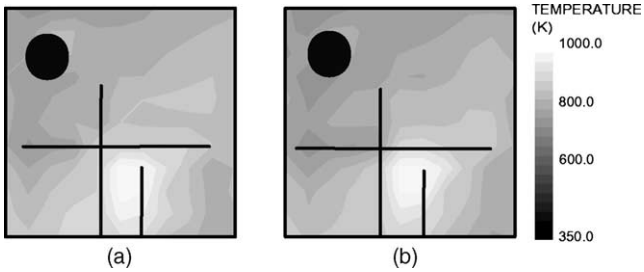

Fig. 4. Predicted (a) and measured (b) temperature distribution for a proposed baffled stove.

temperature profiles. The highest resolution grid had 240 cells along the edges of the cooking surface. The number of cells on the remaining grids were chosen such that the physical location of all the grid points share a location with a grid point on the high resolution grid. This was done to simplify comparison of the temperature profiles. Table 1 shows accuracy and time to convergence as a function of the number of cells.

The accuracy of the models was determined by summing the absolute difference in normalized temperature values at each grid point on the cooking surface and dividing by the number of cells. The temperatures at locations of grid points in the high resolution model that were not present on lower resolution models were determined using Gauss–Seidel iteration.

Fig. 5 shows the error and convergence time for each of the models. Both a stove with no baffles and baffled stove were examined to ensure that the lower resolution model remains a good predictor of performance when baffles are placed in the heating chamber. As shown, the error rises rapidly when the number of cells drops below 40 cells along the edges of the heating chamber, while the time to convergence rises quickly above 30 cells.

Table 1
Number of cells in grid resolution case study models

Number of cells along surface edge	Number of cells for depth of cooking chamber	Total number of cells	Convergence time (s)
240	30	1,949,184	109,845
120	15	233,160	13,199
80	10	76,672	2391
60	10	48,288	1040
48	10	29,952	594
40	10	22,912	497
30	5	11,412	232
24	5	5952	139
20	5	5072	85

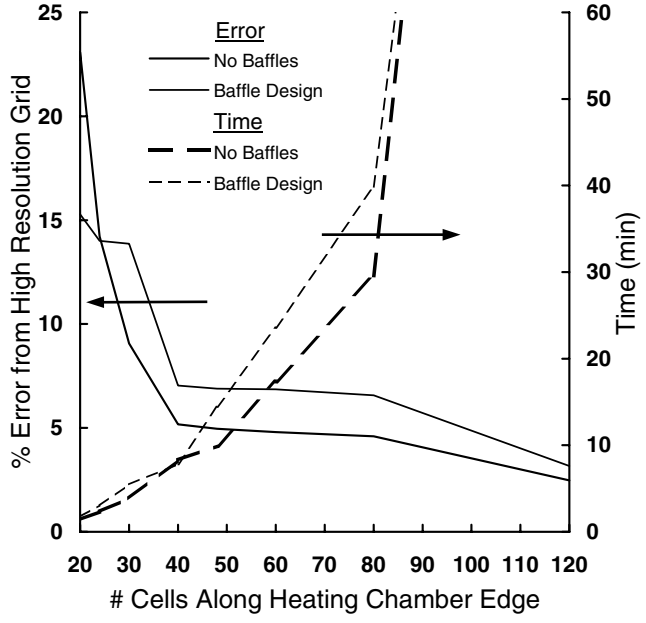

Fig. 5. Accuracy and convergence time as a function of grid size.

As seen in Table 1, the 30 cell stove model tested has only five baffles along the chamber depth while the 40 cell stove has 10. A $30 \times 30 \times 10$ cell model had a surface temperature profile error of 7.6% for the unaltered stove and 11.2% for the baffle stove. The time to convergence was 36 s shorter for the 30 cell unaltered model and 250 s longer for the 30 cell baffle model than the $40 \times 40 \times 10$ model. A $42 \times 42 \times 6$ cell model was examined and resulted in 7.3% and 11.2% error for the unaltered and baffled cell models respectively. However, the convergence time was significantly less (90 s) than the $40 \times 40 \times 10$ model or the $30 \times 30 \times 10$ model. Based on this, the $42 \times 42 \times 6$ model was chosen as the best model for the fitness evaluation. Following completion of the optimization, the proposed solutions were analyzed using high density grids to validate the solution.

To ensure that only designs that can be easily hand-built and produced are considered, baffle orientation is limited to those welded perpendicular to the cooking surface and parallel to the heating chamber walls. Five values are needed to completely describe a baffle's location, length, depth, and orientation. As shown in Fig. 7, the five values are the starting x and y position of the baffle with respect to the lower left corner of the surface, the orientation of the baffle, the length of the baffle, and the depth the baffle penetrates into the flow field. Each of the values are in units of number of cells except baffle orientation, which is determined by an integer between zero and three that represents a baffle moving right, left, up, or down from the starting position. A two-dimensional array is used to represent multiple baffles with the five baffle definition values stored along a column and individual baffles stored in rows. The number of baffles in a particular design was limited to five to ensure the ease of manufacture.

4. Graph based evolutionary algorithms

GBEAs utilize a graph to establish a geography for the population of evolving solutions. The effectiveness and cost of evolved solutions depend on the rate of information transmitted within the population and the population diversity preserved. Many of the designs in small population EAs begin to have the same design features, and valuable diversity is lost. Island EAs (Vekeria and Parmee, 1997; Whitely, 1989) have been successfully used in some applications to overcome this problem. By establishing independent groups of small populations, the solutions can still evolve quickly and

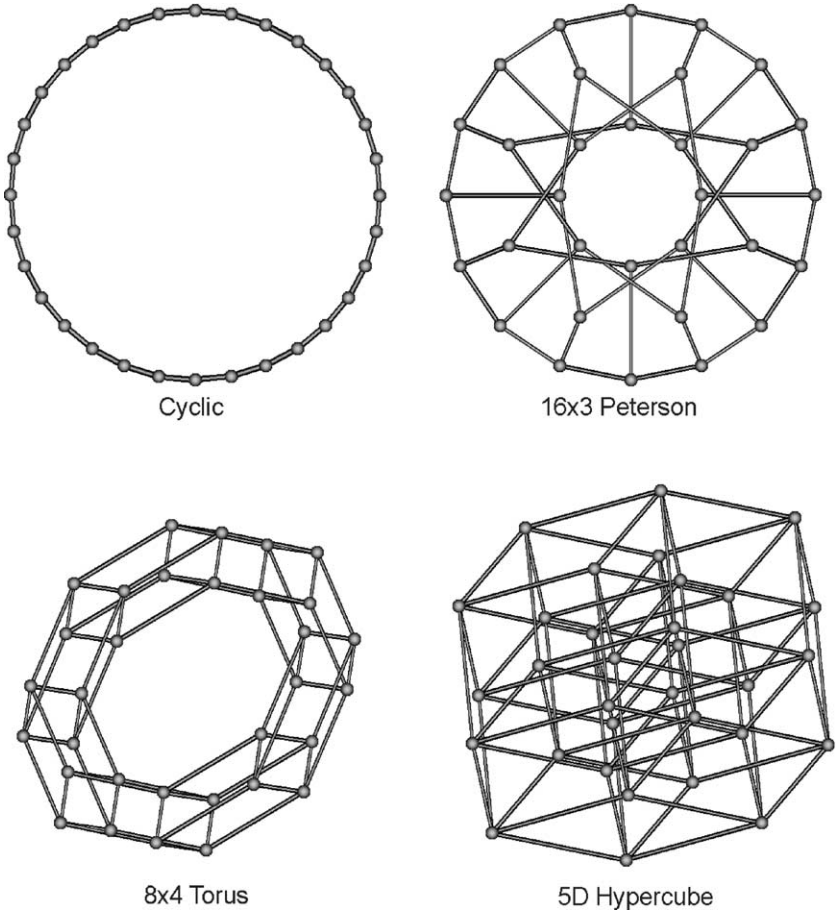

Fig. 6. Graphical topologies used in this study.

still have a chance that innovation will survive. Population graphing is a variation of this technique that also helps maintain diversity in small populations by slowing the early replacement of less fit designs; giving them a chance to evolve before competing with other designs. Population graphing does not, however, require multiple sets of mating rules. In this method, each design in the population is placed on a node in a graphically connected topology for which the design is only allowed to mate with neighboring nodes. Because all designs are members of the same topology, each design still has the opportunity to have an influence on any other design, but the evolution must occur along a path. This gives promising, but less evolved designs extra time to fine-tune and evolve into more fit designs.

Four possible graphs were tested to determine which graph is best for use in this optimization problem. These graphs, shown in Fig. 6, were selected for having different levels of connectivity and for exhibiting diverse behavior in previous EA studies. In order of connectivity from least connected to most are the cycle, 16×3 Peterson, 8×4 torus, and five-dimensional hypercube population graphs. In tournament selection (Miller and Goldberg, 1995) a number of designs are chosen randomly from the entire population. The first design chosen always participates in mating while one other member is chosen randomly from the group in direct proportion to design quality. These two designs then reproduce via the crossover and mutation operators, resulting in two new designs that replace the worst two of the four designs participating in the mating. This results in rapid information spread throughout the population. In contrast, in population graphing mating (Ashlock et al., 1999; Bryden et al., submitted for publication), an initial design is chosen randomly from the population, and the topologically connected neighbors are identified. The initial design then reproduces with a design from the neighbor group in direct proportion to design quality. As in tournament selection, the two new designs replace the two worst from the group consisting of the initial design and its neighboring group. This can significantly slow the rate of information spread.

In both mating schemes, the new designs replacing less fit designs often contain features of the better designs in the mating group. In tournament mating, any design can influence any other less fit design at any time during evolution. In population graphed mating, however, the influence must propagate along the graphical

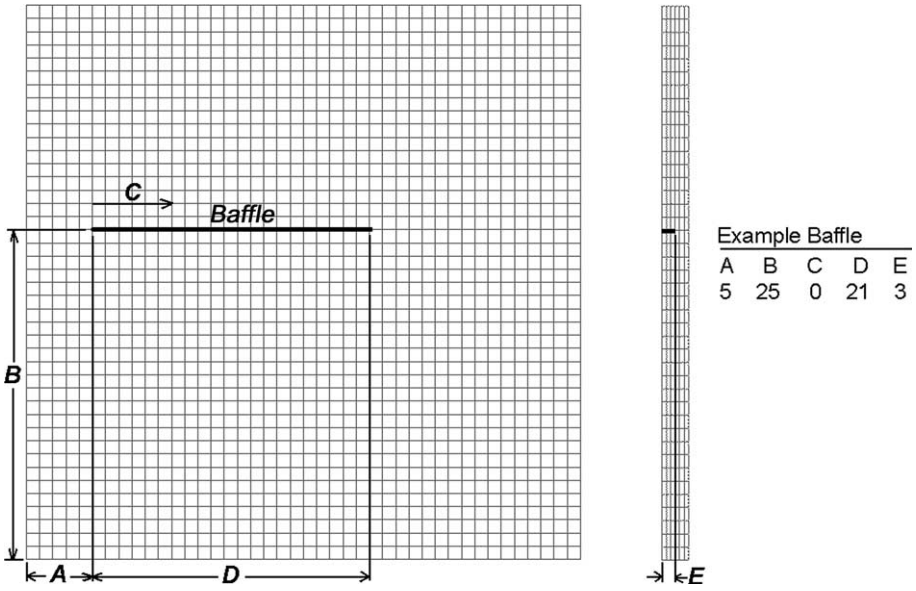

Fig. 7. Baffle structure encoding scheme.

population structure to change remotely located designs, leaving time for other promising solutions to evolve independently. When low connectivity graphs are used, change propagates slowly because there are longer and fewer possible paths to reach another design, leaving more time for independent evolution. With high connectivity, propagation happens more quickly because there are many possible and shorter paths. Additionally, the mating groups for the different graphs are different sizes because nodes have different numbers of neighbors. Because of this, a different percentage of the mating group is replaced in each mating event for different graphs. The effect of this on the efficiency of evolution is problem dependent and is part of the authors' continuing research.

The initial population of designs is generated randomly. Reproduction is simulated in crossover. In crossover, a baffle is chosen at random, and all the baffles later in the baffle list are swapped between the two members. Fig. 8 shows the crossover process used in this algorithm for three baffles. As shown, the point at which crossover can occur in the baffle structure is one of two places either before the second baffle or before the third baffle. In Fig. 8 the last baffle is exchanged between parents 1 and 2 to create the two children. By making small, random changes to the data structures mutation is simulated. There are two types of mutation—baffle mutation and list mutation. In baffle mutation one of the five baffle definition values is chosen randomly from a randomly chosen baffle and replaced with a new value. In list mutation a randomly chosen baffle is replaced with an entirely new random baffle. Population members are chosen randomly to participate in evolution with preference given to the most fit members. The resulting new designs replace the less fit

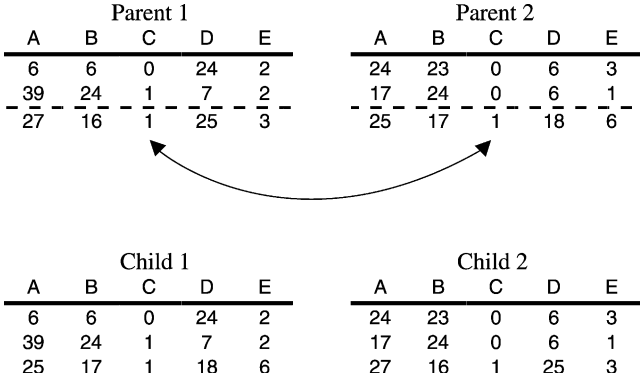

Fig. 8. Diagram of crossover operator.

designs. All baffles were checked following crossover and mutation to ensure that they were sensible; i.e., there were no regions of completely blocked flow and no baffles sticking out of the side of the stove. Baffles that were not sensible were replaced by another baffle created by the same process rather than chopping or other modification. This ensured that the random nature of the baffle mutation was preserved and prevented "building up" baffles at the edge of the design.

5. Fitness function

The fitness function used to assess the evenness of surface temperature is

$$F = \frac{\sum (T_i - T_{\text{avg}})^2}{\sum (T_i - T_{\text{avg}})^2|_{\text{unbaffled}}} \tag{1}$$

where F is the fitness. The values for T_{avg}, the average temperature of the surface, and T_i, the temperature of

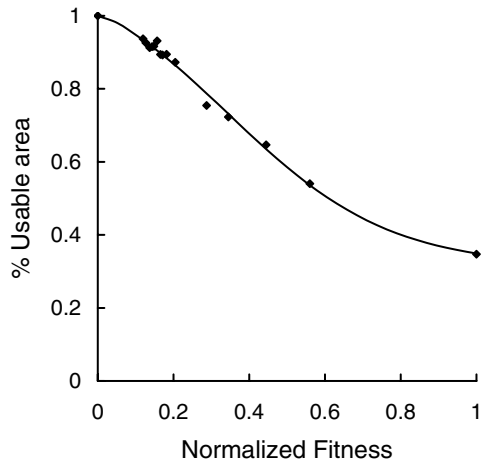

Fig. 9. Usable area as a function of normalized fitness (f).

each of the cells on the cooking surface, are obtained from the CFD solution. In this equation, lower fitness values indicated better solutions. The entire cookstove surface except the area above the flue gas inlet and the area occupied by the chimney are used in the fitness calculation. As shown, the fitness function is normalized by the performance of the unbaffled stove. Because of this, designs with values >1 are worse than the unaltered stove, and designs with values <1 are better than the unaltered stove. A value of 0 indicates a completely even temperature distribution. Fig. 9 shows the approximate relationship between the fitness function and the usable area. The primary purpose of these stoves is for cooking tortillas. Therefore, the more surface area that is available and contiguous within the desired temperature range, the more effective the stove. However, corners do not provide additional cooking area for tortillas, and hence stove effectiveness as a function of cooking area is as shown qualitatively in Fig. 10. If the available cooking area drops too low, no area is large enough to effectively cook tortillas, and there is a point beyond which additional surface area does not result in more effective cooking. Based on this, the optimization process was considered complete when the best design reached a fitness of 0.2. This corresponds to a usable area of approximately 90% and a fully effective stove.

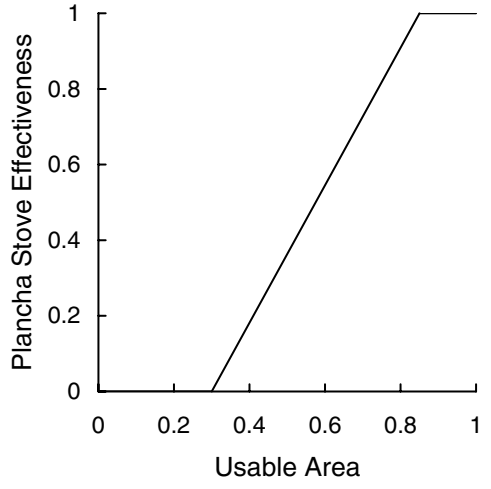

Fig. 10. Plancha stove effectiveness as a function of usable area (f).

6. Implementation and results

For each of the population graphs, four EA runs for 2000 mating events and a population size of 32 members were completed. As noted earlier, the problem was considered solved when the fitness of the best solution dropped below 0.2, at which point the number of mating events were recorded. The computation was continued so that the impact of individual graphs on diversity could be investigated. The best fitness value and the diversity were recorded as a function of mating event. This diversity is used to compare the ability of the graph to maintain a diverse population, and the best fitness value is used to compare the ability of the graph to aid the EA in finding a good solution. The diversity was calculated by normalizing each component of the encoded description of the stove design from 0 to 1 and then calculating the average pair-wise distance between population members of the population by

$$d = \frac{\sum_{q=1}^{32} \sum_{r=q+1}^{32} \left[\sum_{s=1}^{15} (C_{s,q} - C_{s,r})^2 \right]^{1/2}}{[15]^{1/2} \sum_{q=1}^{31} q} \tag{2}$$

where d is diversity, and $C_{s,q}$ is the value of item s of the encoded description for population member q. The measure is normalized by the maximum Euclidean distance for the encoded description, $\sqrt{15}$.

Fig. 11 shows four representative designs obtained from the optimization routine for the hypercube, torus, Peterson, and cycle graphs. On average 90% of the plancha cooking area is within 75 °C of the average temperature, as opposed to 35% of the unaltered stove. Temperature control of the stove surface is based on the feed rate, and the improved design can reach the same cooking temperatures with less fuel, providing a more efficient stove. This occurs because short circuiting of the hot incoming gases to the exhaust chimney is eliminated, reducing the temperature of the exhaust gases and energy loss associated with the exhaust gases.

As shown, all of the baffle structures contain one long, thick baffle blocking the direct flow from inlet to outlet that separates the flow into left-moving and right-moving streams. The two remaining baffles are used to vary the resistance of the two streams. None of the baffles penetrate completely into the flow field. The long baffle and the baffle on the left side of the inlet penetrate 2 cm into the 2.5 cm thick chamber, while the remaining

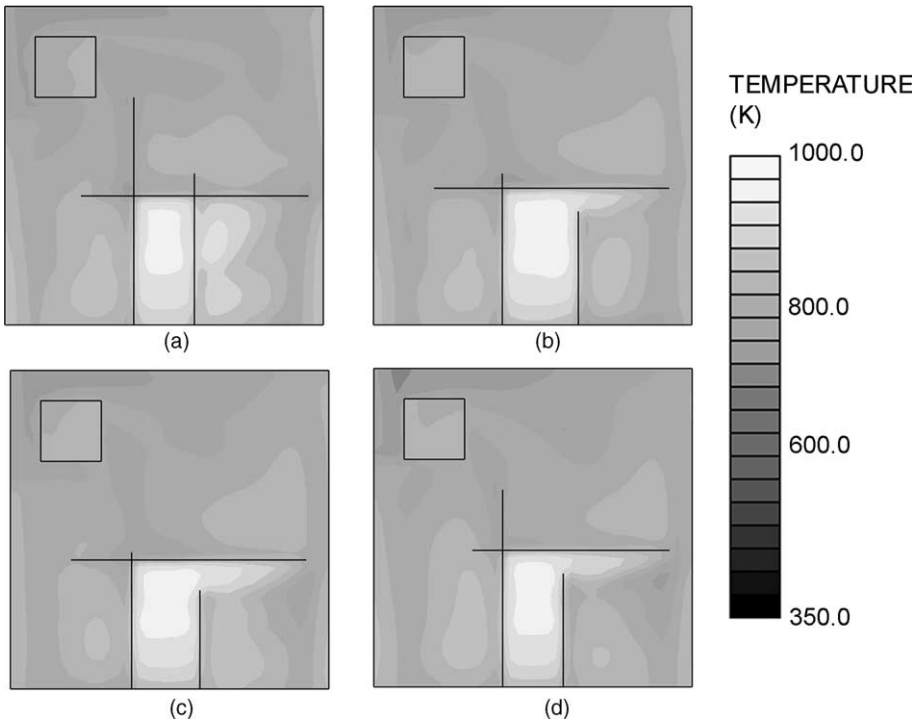

Fig. 11. Representative baffle designs found at $f = 0.2$. Solutions shown were evolved from the cycle (a), Peterson (b), torus (c), and hypercube (d) families. The horizontal and left baffles are 2.0 cm deep in all cases, the right baffle is 1.0, 1.5, 1.5, and 2.0 cm deep for solutions (a), (b), (c) and (d), respectively.

baffle penetrates 1.0–2.0 cm into the flow depending on the design. The common features of these designs suggest that it may be possible to develop a set of guidelines for creating good designs for a variety of sizes and shapes of plancha stoves.

Fig. 12 shows the average of the best fitness for each of the four runs every 20 mating events. Fig. 13 shows the average diversity of the population for the four runs. As shown, the hypercube and torus graphs converge rapidly to a solution while losing significant diversity in the population. The Peterson graph converges next, and the cycle graph converges next. As shown in Table 2, the cycle graph converges in 1160 mating events while the hypercube graph converges in 520, approximately

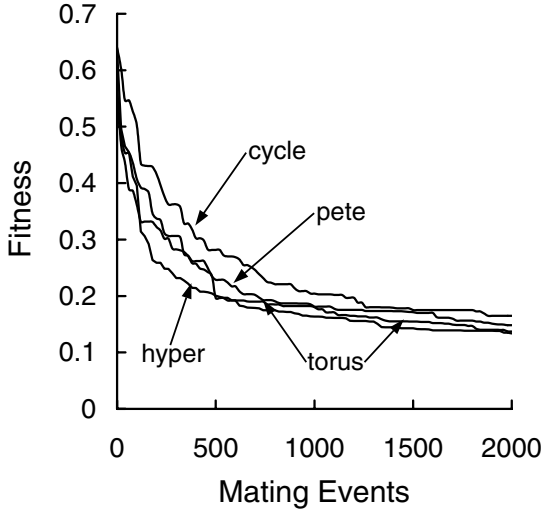

Fig. 12. Normalized fitness (f) of the best population member as a function of number of mating events for each graph family.

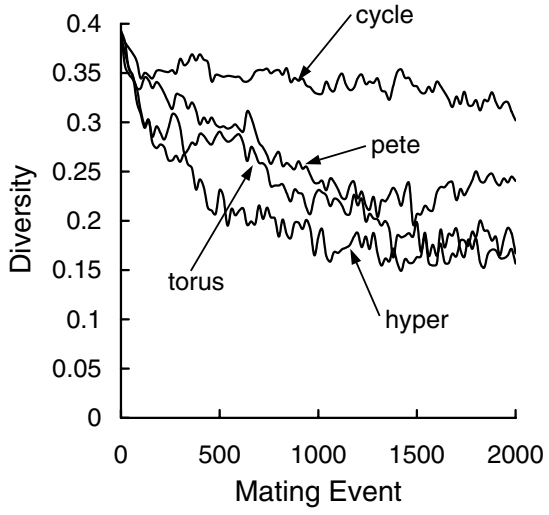

Fig. 13. Diversity (d) of each graph family as a function of mating event.

Table 2
Mean number of mating events for convergence

Graph	Mating events
Cycle	1160
Peterson	720
Torus	520
Hypercube	500

2.25 times faster. The order of convergence matches the degree of connectivity of the graphs—hypercube, torus, Peterson, and cycle—from most connected to least connected. Additionally, the order of convergence is the inverse of the diversity. As shown in Fig. 13, the least diverse population after 2000 runs is the hypercube (diversity coefficient = 0.157), followed by the torus (diversity coefficient = 0.167), the Peterson (diversity coefficient = 0.240), and the cycle (diversity coefficient = 0.302). These results indicate that the earlier results based on simple test cases can be extended to more complex engineering problems of practical interest. The earlier study problems with simple fitness saw significant speedup (10 times or greater) by choosing a highly connected graph. Problems in which the global optimum is composed of the same parts as the local optima had much less speedup (15–20%). In this case the fitness is a mixture of these characteristics, and the results indicate good speedup (2.25 times) using a highly connected graph with performance dropping as connectivity of the graph decreases.

The less connected the graph, the more diverse the population. This diversity is essential in finding the global optimum in very challenging fitness landscapes. In these cases highly disconnected graphs (e.g., cycle graph) permit local good solutions to develop before encountering other locally good solutions and provide a more thorough search of the design space. The persistence of this diversity even after convergence of the GBEA is surprising and highlights the differences in the graphs. The graphs provide a means to tune the ratio of information transmittal and the diversity to minimize the number of mating events to reach a solution. This is particularly useful if some information is known a priori about the fitness landscape, or if the problem will be repeated with differing constraints but with similar fitness landscapes. In the case of this problem, a speedup of 2.25 times reduces the completion time for a single run from approximately eight days to three days on a 24 processor Onyx 2.

7. Summary and future work

GBEAs have been shown to be extendable to a complex, real engineering problem. Particularly in cases in which the fitness function evaluation call is time consuming the computational time can be significantly reduced, by tuning the graph and parameters in a GBEA. In this study the spatial variation of the surface temperature of a plancha stove was minimized. The fitness evaluation routine involved a time consuming call to a CFD program. Because of this, the time savings available are particularly important. However, in many problems, including this one, the shape of the fitness landscape is not known a priori. Additional research work is needed to explore several aspects of GBEAs. These include (1) the development of a simple test or methodology to predict the optimum graph needed for a specific problem, (2) determining if there is a preferred way to select topological neighbors based on the variables used, and (3) the development of ways to control the rate of information spread within a graph. All of these issues require that a measure of connectivity within a GBEA be developed. Currently, there are several measures of connectivity in a graph. The fraction of possible edges present in the graph, the diameter of the graph, the classical connectivity (number of edges required to disconnect the graph), and more exotic measures such as cycle connectivity. None of these measures of connectivity accounts for all the behavioral gradients observed, although diameter tends to correlate best. Development of this new notion of connectivity in the presence of both a selection gradient and variation supplied by mutation and crossover is part of our ongoing research.

Acknowledgements

The help and encouragement of our friends Stuart Conway at Trees, Water, and People and Rogerio Carneiro de Miranda at Proleña–Nicaragua is gratefully acknowledged. We extend our thanks to Dr. Larry Winiarski and Peter Scott, who designed and built the EcoStoves in Nicaragua and gave us the opportunity to work on this problem. We also thank Chris House, an undergraduate at ISU, for building the grid and setting up the code that provided the CFD solutions.

References

Ashlock, D., Schmucker, M., Walker, J., 1999. Graph based genetic algorithms. In: Proceedings of the 1999 Congress on Evolutionary Computation, Washington DC. pp. 1362–1368.

Barnes, D., Openshaw, K., Smith, K.R., van der Plas, R., 1994. What makes people cook with improved biomass stoves? World Bank Technical Paper: Energy Series 242. pp. 1–39.

Bryden, K.M., Ashlock, D.A., Corns, S., submitted for publication. Graph based evolutionary algorithms. IEEE Transaction on Evolutionary Computing.

Blaize, M., Knight, D., Rasheed, K., 1998. Automated optimal design of two-dimensional supersonic missile inlets. Journal of Propulsion and Power 14 (6), 890–898.

Fabbri, G., 1998. Optimization of heat transfer through finned dissipators cooled by laminar flow. International Journal of Heat and Fluid Flow 19 (6), 644–654.

Fan, H.Y., 1998. Inverse design method of diffuser blades by genetic algorithms. In: Proceedings of the Institution of Mechanical Engineers, Part A. Journal of Power and Energy 212 (4), 261–268.

Foster, G.F., Dulikravich, G.S., 1997. Three-dimensional aerodynamic shape optimization and gradient search algorithms. Journal of Spacecraft and Rockets 34 (1), 36–42.

Goldberg, D.E., 1989. Genetic Algorithms in Search, Optimization and Machine Learning. Addison-Wesley, Reading, Maryland.

Hong, C.J., 1994. Health Aspects of Domestic use of Biomass Fuels and Coal in China. Shanghai Medical University, Shanghai, China.

Instituto Nicaragüense de Energia (INE), 1997. Memoria INE 1997, Managua, Nicaragua.

Jang, M., Lee, J., 2000. Genetic algorithm based design of transonic airfoils using Euler equations. In: Collection of Technical Papers—AIAA/ASME/ASCE/ASC Structures, Structural Dynamics and Materials Conference, Atlanta, GA, 1 (2), 1396–1404.

Mäkinen, R., Periaux, J., Toivanen, J., 1999. Multidisciplinary shape optimization in aerodynamics and electromagnetics using genetic algorithms. International Journal for Numerical Methods in Fluids 30 (2), 145–159.

Malhotra, P., 1999. Environmental implications of the energy ladder in rural India. Boiling Point 42, 3–5.

Miller, B.L., Goldberg, D.E., 1995. Genetic algorithms, tournament selection, and the effects of noise. Complex Systems 9 (3), 193–212.

Pandey, M., 1998. Health risk caused by domestic smoke. Boiling Point 40, 6–8.

Poloni, C., Giurgevich, A., Onesti, L., Pediroda, V., 2000. Hybridization of a multi-objective genetic algorithm, a neural network and a classical optimizer for a complex design problem in fluid dynamics. Computer Methods in Applied Mechanics and Engineering 186 (2), 403–420.

Proleña-Nicaragua, 2000. Alternativas Viables Para Solucionar el Problema de Demanda de Leña en la Región Las Segovias. In: Alves-Milho, S.F. (Ed.), Managua, Nicaragua.

Quagliarella, D., Vicini, A., 2001. Viscous single and multicomponent airfoil design with genetic algorithms. Finite Elements in Analysis and Design 37 (5), 365–380.

Schmit, T.S., Dhingra, A.K., Landis, F., Kojasoy, G., 1996. Genetic algorithm optimization technique for compact high intensity cooler design. Journal of Enhanced Heat Transfer 3 (4), 281–290.

Tannehill, J.C., Anderson, D.A., Pletcher, R.H., 1997. Computational Fluid Mechanics and Heat Transfer, second ed. Taylor and Francis, Washington, DC.

Trigg, M.A., Tubby, G.R., Sheard, A.G., 1999. Automatic genetic optimization approach to two dimensional blade profile design for steam turbines. Transactions of the ASME Journal of Turbomachinery 121 (1), 11–17.

Urban, G. 2001. The EcoStove: A case study in thermal system optimization based on differential analysis. Masters thesis, Iowa State University.

Vekeria, H.D., Parmee, I.C., 1997. Reducing computational expense associated with evolutionary detailed design. Proceedings of the 1997 IEEE International Conference on Evolutionary Computation 391-396.

West, D.B., 1996. Introduction to Graph Theory. Prentice Hall, Upper Saddle River, New Jersey.

Whitely, D., 1989. The GENITOR algorithm and selective pressure: Why ranked-based allocation of reproductive trials is best. In: Schaffer, D. (Ed.), Proceedings of the 3d International Conference on Genetic Algorithms. Morgan Kaufmann Publishers, San Francisco, pp. 116–121.

Zha, G., Smith, D., Schwabacher, M., Rasheed, K., Gelsey, A., Knight, D., Haas, M., 1997. High performance supersonic missile inlet design using automated optimization. Journal of Aircraft 34 (6), 697–705.